On the Long-term Equilibrium of Mortality Rates Among Multiple Populations

by

Guangyu Xing

A Thesis submitted to the Faculty of Graduate Studies of

The University of Manitoba

in partial fulfillment of the requirements of the degree of

MASTER OF SCIENCE

Asper School of Business

University of Manitoba

Winnipeg

Contents

List of Tables

List of Figures

On the Long-term Equilibrium of Mortality Rates Among Multiple Populations

Guangyu Xing

June 01, 2016

Abstract

As human life expectancy continues to increase, longevity risk has become a major concern for pension plan sponsors and annuity providers. To hedge the risk, longevity-linked securities have been developed. Since these securities often have payoffs linked to mortality rates of multiple populations, it is important to investigate the relationship between them. In this thesis, we use England and Wales (EW) and Canadian mortality data for illustration. We consider the long-term equilibrium between the mortality indexes of the two populations through cointegration analysis. Our test shows that structural change occurred in the equilibrium. To capture changes in both equilibrium and autoregression structure, we adopt the Threshold Vector Error Correction Model (TVECM). We find that the TVECM model provides adequate fit to our data. This model is further applied to pricing an illustrative longevity bond. Our numerical results indicate that the changes in the long-term equilibrium have a significant impact on longevity bond prices.

Chapter 1

Introduction

1.1 Background

As a recent report produced by World Health Organization (WHO) in 2015 pointed out, we are experiencing a global aging trend nowadays with the global life expectancy rising dramatically from 64 years in 1990 to 71 years in 2013 (shown in Figure 1.1). This phenomenon owes a lot to increasing consciousness of healthy life styles, new medicine, and improving health systems in many countries. Increasing life expectancy is regarded as a good news for human beings. However, this is not the case for annuity providers and pension plan sponsors. For them, they are facing a new emerging risk called longevity risk.

Longevity risk is the risk of people living longer than expected, according to Gavin Jones, the Global Head of Longevity Pricing with Swiss Re in London, UK (JONES, 2013). This risk can cause huge financial burden to annuity providers and pension plan sponsors. Since retirement liability or pension benefit payouts increase with life expectancy, more capitals are required. As a result, how to hedge longevity risk has become an important issue for annuity providers and pension plan sponsors.

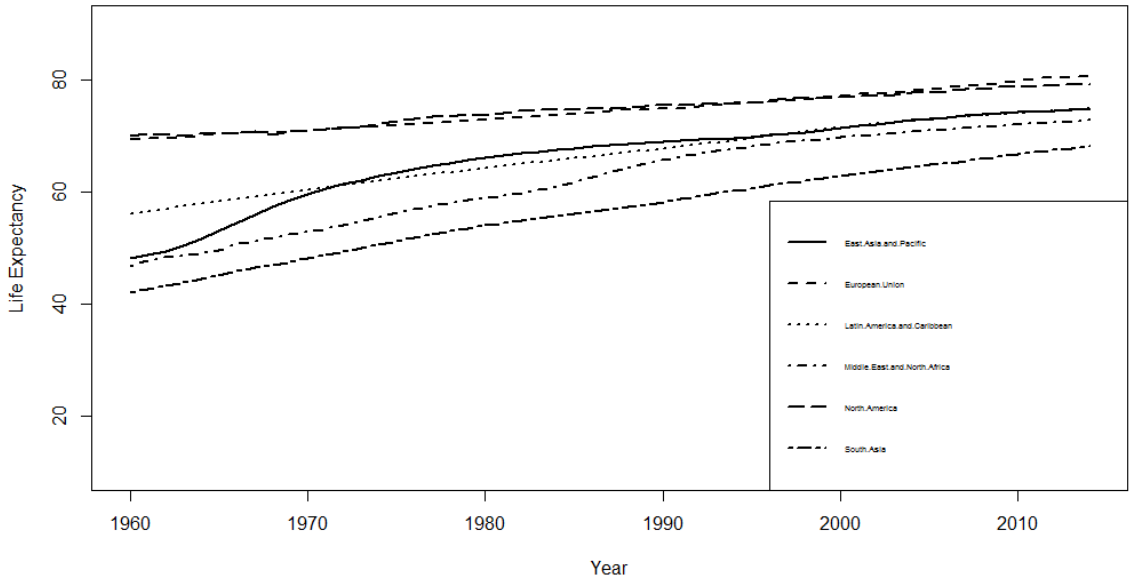

Figure 1.1: Global life expectancy trend

In recent years, the longevity-linked securities have emerged in public for dealing with this issue and rapidly attracted attention from financial institutes. These securities, including bonds, swaps and forwards, are designed to transfer longevity risk to capital markets by linking security payoffs with mortality indexes. For example, in 2007, JP Morgan and Lucida introduced the q-forwards contract which was linked to the mortality rates of 65-year-old males from England and Wales. In 2008, Nathan Ltd issued a mortality bond with payoffs depending on mortality rates of the United States, the United Kingdom, Canada and Germany. In addition, the Kortis Bond, which was issued in December 2010 by Swiss Re, was linked to the divergence in mortality improvement rates between male populations in England and Wales and the United States. As we can see from the observed transactions, longevity-linked securities often involve mortality rate of multiple populations. Investigating the mortality relationships among these populations is the first step towards correctly pricing longevity-linked securities.

1.2 Literature Review

Measuring relationship of mortality rates among multiple populations has interested many researchers and they have proposed a variety of mortality models to deal with it. For example, Carter and Lee (1992) introduced the joint-k model, which assumed that mortality rates of two populations are jointly driven by a single time-varying index. Li and Hardy (2011) compared four extensions to the Lee-Carter model for multiple populations and concluded the Augmented Common Factor model performs better when analyzing a collection of populations including Canada and the United States. Cairns et al. (2011) proposed an Age-Period-Cohort model, which incorporated a mean-reverting stochastic spread that allows for different trends in mortality improvement rates in the short run, but parallel improvements in the long run for two populations. Dowd et al. (2011) introduced a gravity model for the analysis of two related but different sized populations. This is an extension of the Age-Period-Cohort model. They found that the larger the two gravity parameters, the more strongly the smaller population's mortality rates move in line with those of the larger population in the long run. In addition, Jarner and Kryger (2011) used the SAINT model for joint modeling of Danish data and European-wide population data. Danesi et al. (2015) formulated and compared ten multi-population models using data from eighteen Italian regions. Although these methods show advantages of studying multiple population mortality rates, few of them donsider the potential change of long-term equilibrium relationship into consider, as well as the mortality correlations among populations.

One method considering long-term equilibrium relationship is the co-integration analysis. This analysis method is able to separate the potential long-term relationships of variables from their short-term adjustment mechanisms (Kuo et al., 2003). The co-integration analysis was introduced by Engle and Granger (1987) with the model

called Error Correction Model (ECM) dealing with time series for economic studies. It has been used in mortality modeling by several researchers. In univariate studies, for example, Darkiewicz and Hoedemakers (2004) applied cointegration method to test log mortality rates for different ages. Lazar (2004) detected the long term effects using ECM model for Romanian female population. In multivariate studies, the resulting ECM model is usually called Vector Error Correction Model (VECM), for it adds the error correction features to multivariate time series. It is regarded as an effective tool in analyzing multiple population mortality rates. For instance, researchers like Njenga and Sherris (2011) captured the long term equilibrium relationships of mortality rates among populations in Australia, England, Japan, Norway and USA using VECM. Yang and Wang (2013) pointed out that VECM can capture the mortality correlation across countries and enable researchers to derive the analytic form of the survival probability. Zhou et al. (2011) found that VECM gives a better goodness-of-fit and forecasting performance comparing with other models like Vector Auto-Regressive model (VAR) and first order autoregressive process (RWAR). Therefore, using VECM model to detect the long-term equilibrium relationship of mortality rates among multiple populations is reasonable.

When using VECM model, there is concern about possible structural change of the long-term equilibrium relationship. Although the long-term equilibrium relationship can be easily acquired by VECM model, the long time period of mortality data set make it almost impossible for this relationship to work efficiently at each time interval (Seo, 1998). Therefore, we need to test whether the structure of this relationship changes during the time intervals. To test the structural change, Johansen (1991) presented the likelihood methods for the analysis of co-integration as well as the asymptotic distribution of the test statistics. He showed that the asymptotic distribution of the maximum likelihood estimator is mixed Gaussian and one can conduct inference on the

co-integrating relations using the Chi-square distribution. Hansen (2003) generalized the test for more than one structural changes. He found the asymptotic distribution is also Chi-square distribution, but he applied the testing method in univariate case, the US term structure data. For multivariate structural change test, Seo (1998) proposed Lagrange Multiplier (LM) test. More specifically, in cointegrated systems he tested whether cointegrating vector changes, or the adjustment vector changes, or both of them change jointly with an unknown change point. Furthermore, he also presented the test statistic and asymptotic distributions for all situations.

In VECM model, the long-term equilibrium relationship is expressed in a linear form. However, if structural change happens, it will be not proper to describe the relationship in a linear form. Several models have been proposed for measuring the non-linear behavior. One is Markov switching model, which is first proposed by Goldfeld and Quandt (1973) in economic field. This model involves multiple structures that can characterize the time series behaviors governed by Markov chain in different regimes. In cointegration systems, the Markov Switching Vector Error Correction Model (MSVECM) is first proposed by Krolzig et al. (1996) by allowing the equilibrium errors follow Markov process. However, transition probabilities in MSVECM does not depend on which state the deviation was in before. Another popular model is Threshold Vector Error Correction Model (TVECM). Balke and Fomby (1997) introduced the concept of threshold co-integration, which takes the deviation from the long-term equilibrium into consideration. Their initial goal is to consider the presence of transaction costs in economic field. This model soon becomes popular and has been used in analyzing various economic terms. However, it is still new in mortality field. In the TVECM model, the time series are cointegrated if they move far away from equilibrium relationship. If they are vary close to the equilibrium, they are not cointegrated. This behavior is usually measured by the deviation from the equilibrium relationship (the

deviation in VECM model), that whether it is beyond or below some threshold values. The test for threshold cointegration is often broken into two steps: testing the cointegration relationship similar as in VECM model, and then testing the threshold effect of the deviation. The TVECM model is usually estimated by maximum likelihood method, as proposed by Hansen and Seo (2002).

1.3 Objective

In this thesis, we would like to investigate the long-term equilibrium relationship among multiple population's mortality rates. We use the mortality rates of England and Wales', and Canadian total populations for illustration to test their long-term equilibrium relationship. To achieve this goal, we first use VECM model to find the relationship, then perform the structural change test. After that, we re-estimate the relationship by using TVECM model. We then forecast the mortality rates for both populations.

Another objective of this thesis is to price a longevity bond using TVECM model. The bond used for illustration is analogous to the Kortis bond, issued by Swiss Re in December 2010. The illustrative bond is used for hedging the longevity risk of an insurance company that sells annuity policies in England and Wales and life insurance policies in Canada. We use multivariate Wang transform to price the bond and compare the bond prices using TVECM and VECM model.

The reminder of the thesis is organized as follows: Chapter 2 introduces the data set and the mortality model we use. Chapter 3 tests the long-term equilibrium relationship using VECM model. Chapter 4 tests the structural change of the relationship. Chapter 5 we re-estimate the equilibrium relationship using TVECM model. Chapter 6 applies TVECM model to longevity bond pricing. Chapter 7 concludes.

Chapter 2

Mortality Model

Most analysis of mortality rates uses models which decompose mortality rates into dimensions, including age, period or other variables, rather than using mortality rates directly. These variables explain how mortality rates change in a natural way. In this chapter, we first introduce the mortality model that we are going to use. Next, when applied by our mortality model, we will give a description of our data set.

2.1 Lee-Carter Model

According to Hunt and Blake (2015), the first and still the most widely used mortality model is Lee-Carter model, which is first proposed in Lee and Carter (1992). Since then, it has been suggested by many researchers and also been recommended for use by the US Bureau of the Census as a benchmark model (Mitchell et al., 2013). Therefore, we will use this classic mortality model in our research.

The Lee-Carter model is expressed as:

$$\ln(m_{x,t}) = a_x + b_x k_t + e_{x,t}, \tag{2.1}$$

where $m_{x,t}$ is the central mortality rate for a life aged x at time t; a_x is the age effect describing the general shape of the mortality schedule; b_x is age-sensitivity with respect to the changes in fixed k_t; k_t is the time-varying index signifying the general speed of mortality improvement and capturing the main time trend for all ages, and it is sometimes referred as mortality index; $e_{x,t}$ is the error term reflecting the influences not captured by the model. In the original Lee-Carter model, the error term follows normal distribution with mean zero and an age-specific variance σ_x. In this paper, we follow Yang and Wang (2013) and let the change in error terms follow a Markov stochastic process. $\Delta e_{x,t}$ and $\Delta e_{x,s}(s \neq t)$ are assumed to be independent, where $\Delta e_{x,t} = e_{x,t} - e_{x,t-1}$, $\Delta e_{x,t}$ follows normal distribution with mean zero and variance equal to σ_x.

2.2 Fitting the Model

Lee and Carter (1992) suggested Singular Value Decomposition (SVD) to fit Lee-Carter model for the data.

Identification constraints are required to obtain unique estimates of a_x, b_x and k_t. The reason is that, k_t is determined up to a linear transformation; b_x is determined to a multiplicative constant, and a_x is determined up to an additive constant; as Lee and Carter (1992) pointed out. In order to derive a unique solution, we impose the following constraints: $\sum b_x = 1$ and $\sum k_t = 0$. a_x is simply set to the average of $\ln(m_{x,t})$ over the sample period.

2.3 Data Description

We use total population mortality rates of England and Wales (EW), and Canada (CAN) aged 50 to 89 from year 1925 to 2011. The mortality rates are acquired from Human Mortality Database (2015).

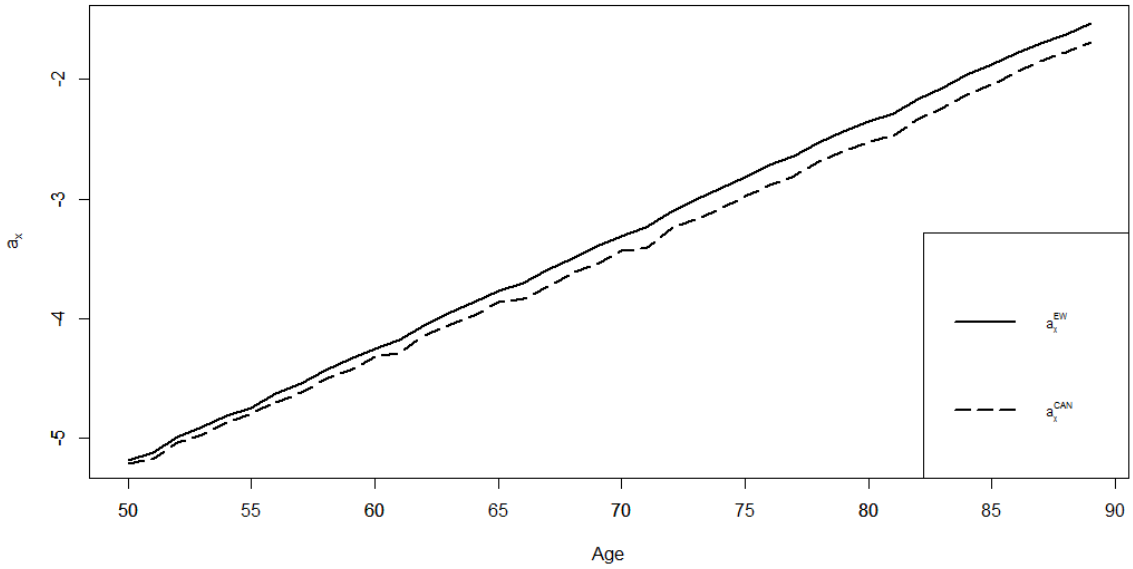

Figure 2.1: a_x of EW and CAN

We fit EW and CAN mortality rates using Lee-Carter as described in section 2.2, parameter estimates of a_x and b_x are depicted in Figure 2.1 and Figure 2.2. From now on, we add superscript "EW" and "CAN" to a_x, b_x and k_t to distinguish the parameters for the two models for EW and CAN. As the Figure 2.1 shows, both a_x^{EW} and a_x^{CAN} increase steadily as the age rises, indicating average mortality rates increase with age. a_x^{EW} is lower than a_x^{CAN}, indicating that the EW has lower mortality rate than CAN for the same age group. In Figure 2.2, the decreasing trend of b_x tells us mortality rates at older ages are less sensitive to the changes of k_t.

Figure 2.3 plots the mortality index k_t^{EW} and k_t^{CAN} from 1925 to 2011. Both k_t^{EW}

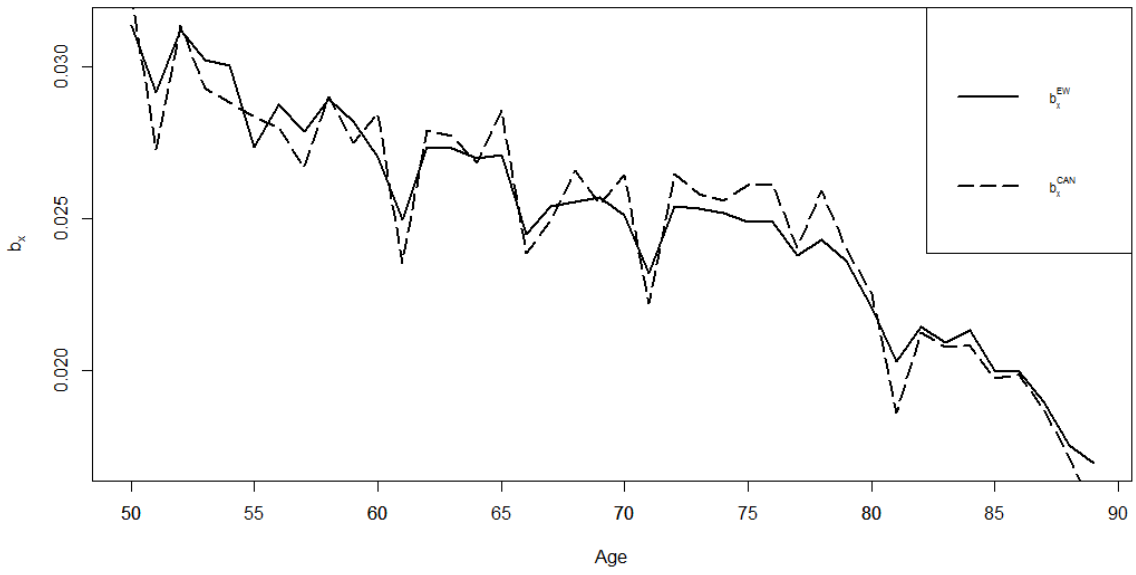

Figure 2.2: b_x of EW and CAN

and k_t^{CAN} generally decline during this sample period, implying that mortality rates are decreasing in both regions. Figure 2.3 also shows a large fluctuation of mortality rates in both countries from year 1930 to 1945 due to the two World Wars. This is especially apparent in k_t^{EW}.

More specifically, it appears that k_t^{EW} and k_t^{CAN} are following the same trend. Their trajectory cross with each other several times over the sample period. For example, from 1950 to 1970 they appear to cross each other; from 1970 they start to diverge; from 1990 they cross again. Hence we would like to investigate whether there exists a long-term equilibrium relationship between the two and what the relationship looks like.

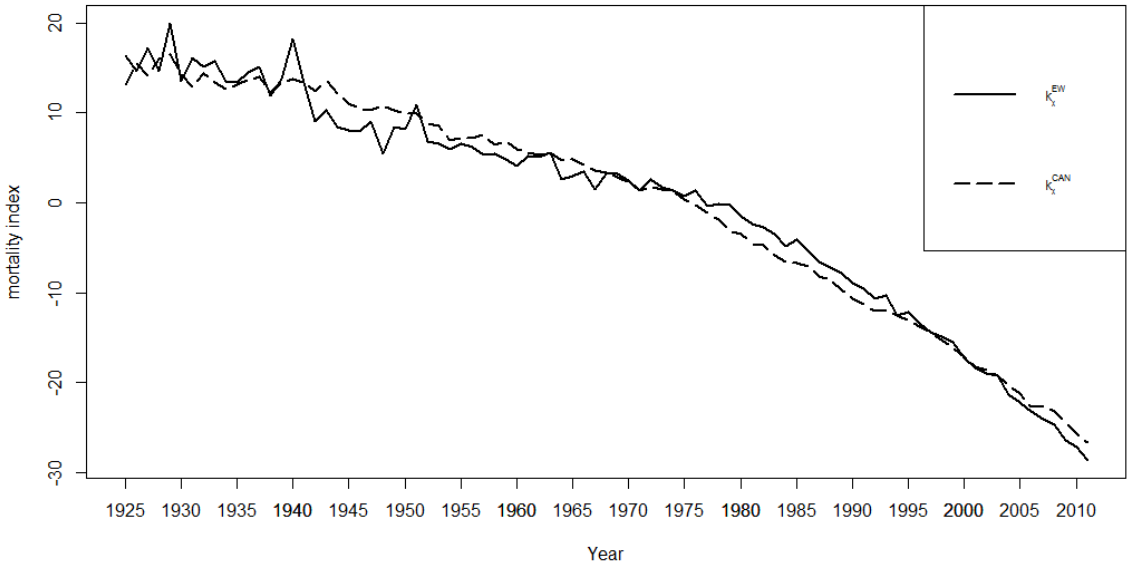

Figure 2.3: Historical Mortality Index of EW and CAN

Chapter 3

Vector Error Correction Model

In this chapter, we model k_t^{EW} and k_t^{CAN} and investigate the long term equilibrium relationship of between the two using VECM model. This chapter is organized as follows: first, we describe the cointegration analysis; next, we introduce VECM model; finally we do the empirical study.

3.1 Cointegration Analysis

Cointegration is an economic concept which mimics the existence of a long-term equilibrium among economic time series. A time series data y_t is called integrated if its first difference $\Delta y_t = y_t - y_{t-1}$ is stationary (y_t is $I(1)$). If two or more integrated time series data have a stationary linear combination, then they are called cointegrated. Mathematically, the definition is:

Given a set of *I(1)* variables $\mathbf{k} = \{k_t^{EW}, k_t^{CAN}\}$, if there exists a linear combination with a vector $\boldsymbol{\beta}$ and $\boldsymbol{\beta} \neq 0$ such that

$$\beta_1 k_t^{EW} + \beta_2 k_t^{CAN} \sim I(0),$$

then the **k**'s are cointegrated. Note that $I(0)$ denotes stationary time series.

In this case, the time series data are driven by a common trend and the variations of the variables are correlated with each other. This common trend is what we called "long-term equilibrium".

To apply cointegration analysis in time series, the following procedures are used: (1) Make sure each time series is nonstationary, and their first difference is stationary. (2) Examine whether the linear combination of the two time series is stationary.

3.2 VECM model

Vector Error Correction Model (VECM) is a special case of Vector Auto-Regressive (VAR) model with cointegration relationship taken into consideration. In this model, the changes in time series also depend on the deviation from the equilibrium relationship. VECM model can be written in the VAR form. The VAR model for k_t^{EW} and k_t^{CAN} can be expressed as:

$$\begin{pmatrix} k_t^{EW} \\ k_t^{CAN} \end{pmatrix} = c + \Phi_1 \begin{pmatrix} k_{t-1}^{EW} \\ k_{t-1}^{CAN} \end{pmatrix} + \Phi_2 \begin{pmatrix} k_{t-2}^{EW} \\ k_{t-2}^{CAN} \end{pmatrix} + ... + \Phi_p \begin{pmatrix} k_{t-p}^{EW} \\ k_{t-p}^{CAN} \end{pmatrix} + \begin{pmatrix} \varepsilon_t^{EW} \\ \varepsilon_t^{CAN} \end{pmatrix}, \quad (3.1)$$

The VECM form of equation (3.1) is expressed as:

$$\begin{pmatrix} \Delta k_t^{EW} \\ \Delta k_t^{CAN} \end{pmatrix} = c + \Pi \begin{pmatrix} k_{t-1}^{EW} \\ k_{t-1}^{CAN} \end{pmatrix} + \sum_{i=1}^{p-1} \Gamma_i \begin{pmatrix} \Delta k_{t-i}^{EW} \\ \Delta k_{t-i}^{CAN} \end{pmatrix} + \begin{pmatrix} \varepsilon_t^{EW} \\ \varepsilon_t^{CAN} \end{pmatrix}, \quad (3.2)$$

where c is a 2×1 constant vector; Π is a 2×2 long term loading matrix; Γ_i is a 2×2 short-term loading matrix for $i = 1, 2, ..., p$; p is the lag order; and $\begin{pmatrix} \varepsilon_t^{EW} \\ \varepsilon_t^{CAN} \end{pmatrix}$ follows bivariate normal distribution.

The rank of Π indicates whether k_t^{EW} and k_t^{CAN} have cointegration relationship. If the rank of Π is 0, then there is no long-term equilibrium. If the rank of Π is full rank, then the original time series must be stationary. Since we only have two time series in our study, the full rank is 2. Only when the rank of Π is greater than 0 but less than full rank (equal to 1 in our case), there exists cointegration relationship. Under this condition, the long term loading matrix Π can be further factorized as $\Pi = \alpha\boldsymbol{\beta}'$. By following a constant term in the cointegration relationship, the general form of VECM model is expressed as follows:

$$\begin{pmatrix} \Delta k_t^{EW} \\ \Delta k_t^{CAN} \end{pmatrix} = c + \alpha\left(k_{t-1}^{EW} - \beta k_{t-1}^{CAN} + w\right) + \sum_{i=1}^{d} \Gamma_i \begin{pmatrix} \Delta k_{t-i}^{EW} \\ \Delta k_{t-i}^{CAN} \end{pmatrix} + \begin{pmatrix} \varepsilon_t^{EW} \\ \varepsilon_t^{CAN} \end{pmatrix}, \quad (3.3)$$

where w is the constant term in long-term equilibrium; α is adjustment coefficient (2×1 vector); β is cointegrating value, comes from the normalized cointegration vecter $\boldsymbol{\beta}' = (1, \beta)$.

Equation (3.3) shows how VECM model incorporates both the long-term equilibrium relationship and the short-term relationship. In the long run, the two time series are expected to follow the relationship $k_t^{EW} - \beta k_t^{CAN} + w = 0$. If there is deviation from this equilibrium, the correction term $\alpha(k_t^{EW} - \beta k_t^{CAN} + w)$ pulls the time series towards the equation. This is why we called the model as "error correction" model.

Generally, the procedures of estimating VECM model include four steps:

1. Ensure that k_t^{EW} and k_t^{CAN} follows $I(1)$ process.

2. Determine the lag order of the VAR model, and VECM model will have 1 less lag.

3. Perform cointegration tests to examine if there exists cointegration relationship.

4. Estimate the VECM model.

First, to check whether the two time series are $I(1)$ process, we use the Dickey-Fuller (DF) test. DF test is designed for testing the existence of unit root, and the existence of unit roots indicating the time series is non-stationary. The null hypothesis of DF test is that unit roots exist. Since DF test is a left-tailed test, we expect that for $I(1)$ process, the null hypothesis is accepted for the original time series and rejected for the first order difference of the time series. In another word, we expect k_t^{EW} and k_t^{CAN} to be non-stationary processes but their first order difference to be stationary.

Second, to choose the lag order, we use four criteria: Akaike Information Criteria (AIC), Hannan–Quinn Information Criteria (HQ), Schwarz Information Criteria (SC) and Final Prediction Error Criteria (FPE). The four criteria are calculated as following:

$$AIC(p) = \ln|\Sigma(p)| + \frac{2}{T}pQ^2$$

$$HQ(p) = \ln|\Sigma(p)| + \frac{2\ln\ln T}{T}pQ^2$$

$$SC(p) = \ln|\Sigma(p)| + \frac{\ln T}{T}pQ^2$$

$$FPE(p) = \left[\frac{T + Qp + 1}{T - Qp - 1}\right]^Q |\Sigma|$$

where p is the lag order; $\Sigma_{(p)}$ is the maximum likelihood (ML) estimator of the covariance matrix for a VAR(p) model; T is the sample size; and Q is the number of parameters. The lower the criteria values, the better goodness of fit. Notice that we determine the lag order for VAR model, and then deduct the order by 1 for VECM model.

Third, to test whether k_t^{EW} and k_t^{CAN} have cointegration relationship, we apply the widely used method, Johansen test. Johansen test is designed for testing the number of ranks in Π. Only when the rank number equals 1, will k_t^{EW} and k_t^{CAN} have cointegration relationship. There are two forms of Johansen test: Maximum Eigenvalue test and Trace test. The Maximum Eigenvalue test tests rank= r against rank= $r+1$, while Trace test is to test rank= r against rank> r.

Finally, the parameters in VECM can be estimated by maximum likelihood method (MLE).

3.3 Numerical Results

Table 3.1 shows the DF test results of k_t^{EW} and k_t^{CAN}, and Δk_t^{EW} and Δk_t^{CAN} results, respectively. As Table 3.1 shows, both k_t^{EW} and k_t^{CAN} are non-stationary time series, because the test statistics are greater than the critical value at 10%, 5% and 1% significance level. Δk_t^{EW} and Δk_t^{CAN} are stationary time series, since the test statistic are all smaller than the critical values. Therefore, both k_t^{EW} and k_t^{CAN} are $I(1)$ process.

Data	**Test Statistic**	**Critical Value**		
		Sig=0.01	Sig=0.05	Sig=0.1
k_t^{EW}	1.5752	-2.6	-1.95	-1.61
k_t^{CAN}	1.7268			
Δk_t^{EW}	-7.054			
Δk_t^{CAN}	-4.6294			

Table 3.1: Dickey-Fuller Test Result

Table 3.2 shows the AIC, HQ, SC and FPE values for various lag order. Lag order 4 has the lowest AIC, HQ and FPE, while lag order 3 has the lowest SC. We further perform a Likelihood Ratio test for VAR(3) against VAR(4), and the test result shows VAR(3) is rejected. Hence we choose lag order 4 for VAR model, which indicates lag order 3 for VECM.

	1	2	3	4	5
AIC	-0.1813386	-0.292597	-0.435695	**-0.496567**	-0.437663
HQ	-0.1106366	-0.174761	-0.270723	**-0.284461**	-0.178422
SC	-0.0052372	0.000904	**-0.024792**	0.0317369	0.208042
FPE	0.8342073	0.746548	0.647353	**0.609697**	0.647647
LR test of VAR(3) against VAR(4)	Test Statistic: 29.994289 > Critical Value: 9.487729				

Table 3.2: Lag Order Selection Results for VAR Model

Table 3.3 shows the results of Johansen tests. Both p-value are smaller than 0.05 for trace test and eigenvalue test when testing rank number equal to 1. When testing rank number equal to 0, both p-value are high, and thus we reject the null hypothesis. Based on the test results, the rank number is 1 for our data set at 1% significant level. Therefore, we conclude that k_t^{EW} and k_t^{CAN} are cointegrated.

Rank	**Trace statistic**	**p-value**	**Eigen statistic**	**p-value**
0	22.522427	0.003032	20.34578	0.003844
1	2.176647	**0.140119**	2.176647	**0.140118**

Table 3.3: Johansen test for cointegration relation between k_t^{EW} and k_t^{CAN}

Finally, the VECM model is estimated by MLE and the estimated model is shown below:

$$\begin{aligned}
\begin{pmatrix} \Delta k_t^{EW} \\ \Delta k_t^{CAN} \end{pmatrix} &= \begin{pmatrix} -0.703 \\ -0.58 \end{pmatrix} + \begin{pmatrix} -0.1509 \\ -0.011 \end{pmatrix} \left(k_{t-1}^{EW} - 0.992 k_{t-1}^{CAN} + 0.4616 \right) \\
&+ \begin{pmatrix} -0.4189 & 0.3024 \\ -0.017 & -0.0631 \end{pmatrix} \begin{pmatrix} \Delta k_{t-1}^{EW} \\ \Delta k_{t-1}^{CAN} \end{pmatrix} + \begin{pmatrix} -0.1817 & -0.4204 \\ 0.0016 & -0.1636 \end{pmatrix} \begin{pmatrix} \Delta k_{t-2}^{EW} \\ \Delta k_{t-2}^{CAN} \end{pmatrix} \\
&+ \begin{pmatrix} -0.2475 & 0.5699 \\ 0.0407 & 0.0629 \end{pmatrix} \begin{pmatrix} \Delta k_{t-3}^{EW} \\ \Delta k_{t-3}^{CAN} \end{pmatrix} + \begin{pmatrix} \varepsilon_t^{EW} \\ \varepsilon_t^{CAN} \end{pmatrix}.
\end{aligned} \tag{3.4}$$

From equation (3.4), we find that in the long run $k_{t-1}^{EW} = 0.992k_{t-1}^{CAN} - 0.4616$. The deviation from $k_t^{EW} - 0.992k_t^{CAN} + 0.4616$ will be multiplied by the adjustment coefficient. For example, if k_{t-1}^{EW} is great larger than $0.992k_{t-1}^{CAN} - 0.4616$ in the year $t-1$, the deviation from the equilibrium is a positive number. For Δk_t^{EW}, the deviation is multiplied by -0.1509, while for Δk_t^{CAN}, the deviation is multiplied by -0.011. This reduces both k_t^{EW} and k_t^{CAN} in the year t. However since $\mid -0.1509 \mid > \mid -0.011 \mid$, it reduces k_t^{EW} more than k_t^{CAN}. Therefore in year t the difference between k_t^{EW} and k_t^{CAN} shrinks. That is how the error correction term works and how the two time series converge to the long term equilibrium. In addition, the reason why the adjustment speed of k_t^{EW} is faster than k_t^{CAN} could be that k_t^{EW} fluctuates more than k_t^{CAN} (as shown in Figure 2.3), so so the extent of correction is larger.

Finally, we check autocorrelation and normality of the residuals from the estimated VECM model. When checking autocorrelation, we use lag order from 1 to 10. Table 3.4 shows there is no autocorrelation in the residuals of VECM model, since all p-value are large.

Lag	**Statistic**	**p-value**
1	1.79	0.78
2	4.17	0.80
3	6.23	0.84
4	10.51	0.71
5	14.34	0.63
6	17.46	0.62
7	20.57	0.62
8	24.54	0.56
9	28.58	0.51
10	32.08	0.50

Table 3.4: Results of Checking Auto-correlation in Residuals from VECM model

	Test statistic	**p-value**
Mardia's Test (skew)	0.6813	0.071
Mardia's Test (kurtosis)	10.8636	0.0018
Henze-Zirkler Test	1.5316	0.0012

Table 3.5: Results of Checking Normality of Residuals from VECM model

When checking the normaltiy ofresiduals, we use three multivariate normality test: Mar-

dia's test for testing skewness, Mardia's test for testing kurtosis and Henze-Zirkler test. Table 3.5 summerizes the test results. It shows that the residuals are not normality distributed, because all p-value are very small and thus we reject the null hypothesis of normal distribution. Therefore, VECM model does not adequately fit our data. In the next chapter, we will consider structural change in the long-term equilibrium by testing the constancy of adjustment coefficient and the cointegration value, and then adjust the model accordingly.

Chapter 4

Structural Change

4.1 Langrange Multiplier Test

When testing for structural change in cointegration system, we are interested in whether the adjustment coefficient α changes, or the cointegration vector $\boldsymbol{\beta}$ changes, or both change during the sample period. Seo (1998) presented how to test structural change in cointegration system using Langrange Multiblier (LM) test. It does not only work for a known change point, but also work for an unknown change point which is more common in researches. In addition, Seo (1998) derived the test statistic and asympototic distribution for testing changes in α, $\boldsymbol{\beta}$ and $\alpha\boldsymbol{\beta}^{'}$. The test is based on the maximum likelihood estimator (MLE) of the cointegration model.

Assume that break point, τ, is known and $\tau \in (0,1)$. It seperates the sample period into two subsamples, $t = 1, 2, ...[n\tau]$ and $t = [n\tau] + 1, [n\tau] + 2, ..., n$. $\boldsymbol{\beta}$ changes to $\boldsymbol{\beta} + \delta$ after the break point. The null hypothesis of the test is $\delta = 0$ indicating stability of $\boldsymbol{\beta}$, while the alternative hypothesis is $\boldsymbol{\beta} \neq 0$. The log-likelihood function with one breaking point is given by:

$$L^{\beta}(\theta, \tau) = \sum_{t=1}^{[n\tau]} l_t(0, \boldsymbol{\beta}, \alpha, \Gamma, \Sigma) + \sum_{[n\tau]+1}^{n} l_t(\delta, \boldsymbol{\beta}, \alpha, \Gamma, \Sigma), \tag{4.1}$$

where

$$l_t(\theta) = -\frac{1}{2}\log|\Sigma| - \frac{1}{2}\mathrm{tr}\{\varepsilon_t(\theta)\varepsilon_t^{'}(\theta)\Sigma^{-1}\},$$

and θ is parameter vector and $\theta = (\delta, \boldsymbol{\beta}, \alpha, \Gamma, \Sigma)$; Σ is the variance-covariance matrix of the residuals in VECM model; other parameters are the same as defined in VECM model before. The LM test statistic for the null hypothesis is :

$$\mathrm{LM}_n^{\boldsymbol{\beta}}(\tau) = \lambda_n^{\boldsymbol{\beta}^{'}}(\tau)[Est.Var(\lambda_n^{\boldsymbol{\beta}}(\tau))]^{-1}\lambda_n^{\boldsymbol{\beta}}(\tau), \tag{4.2}$$

where $\lambda_n^{\boldsymbol{\beta}}(\tau)$ is the Lagrange multiplier (or the score), and it is the vector of the first partial derivative of the log-likelihood function (4.1) with respect to each parameter. $Est.Var$ is short for estimated variance. Asymptotic critical values of the test statistic is calculated by simulation method and provided by Seo (1998).

If the adjustment coefficient changes during the sample period, then the value of α changes to $\alpha + \epsilon$ after the break point. The null hypothesis of testing the stability of α is $\epsilon = 0$ and the alternative hypothesis is $\epsilon \neq 0$. The log-likelihood function incorporating the change is written as:

$$L^{\alpha}(\theta, \tau) = \sum_{t=1}^{[n\tau]} l_t(0, \boldsymbol{\beta}, \alpha, \Gamma, \Sigma) + \sum_{[n\tau]+1}^{n} l_t(\epsilon, \boldsymbol{\beta}, \alpha, \Gamma, \Sigma), \tag{4.3}$$

and the corresponding LM test statistic is:

$$\mathrm{LM}_n^{\alpha}(\tau) = \lambda_n^{\alpha^{'}}(\tau)[Est.Var(\lambda_n^{\alpha}(\tau))]^{-1}\lambda_n^{\alpha}(\tau), \tag{4.4}$$

where $\lambda_n^{\alpha}(\tau)$ is the vector of first partial derivative of the log-likelihood function with respect to each parameter.

If both α and $\boldsymbol{\beta}$ change jointly during the sample period, the LM test statistic is simply the sum of Equation (4.2) and Equation (4.4):

$$\mathrm{LM}_n^{\alpha\boldsymbol{\beta}}(\tau) = LM_n^{\alpha}(\tau) + LM_n^{\boldsymbol{\beta}}(\tau). \tag{4.5}$$

When the break point is unknown, the testing procedure is nonstandard because τ only appears under the alternative hypothesis. According to Andrews (1993) and (1994)Andrews and Ploberger (1994), three kinds of LM test statistics can be used for testing structural change with unknown break points: average (Ave-LM), exponential average (Exp-LM) and supremum (Sup-LM) statistics. Assume the break point τ lies in the sample period of $[\underline{\tau}, \overline{\tau}]$, the LM test statistics are expressed as:

$$\text{Ave} - \text{LM}_n^i = \frac{1}{\overline{\tau} - \underline{\tau}} \sum_{t=\underline{\tau}}^{\overline{\tau}} \text{LM}_n^i([t/n]), \tag{4.6}$$

$$\text{Exp} - \text{LM}_n^i = \log\left(\frac{1}{\overline{\tau} - \underline{\tau}} \sum_{t=\underline{\tau}}^{\overline{\tau}} \exp\Big(\text{LM}_n^i([t/n])/2\Big)\right), \tag{4.7}$$

$$\text{Sup} - \text{LM}_n^i = \max_{t\in[\underline{t},\overline{t}]}\Big(\text{LM}_n^i([t/n])\Big), \tag{4.8}$$

where $i = \alpha, \boldsymbol{\beta}$ and $\alpha\boldsymbol{\beta}$.

The difference of the three is the power of statistic (Seo, 1998). In this thesis, we will calculate all three statistics. The null hypothesis is rejected if the test statistics are greater than the critical values and vice versa.

4.2 Structural Change Testing Results

We apply LM test by assuming break point τ lines in [0.05, 0.95]. It is reasonable to assume the break point occurred in a wide range, for a wider range captures more possible structural changes. However, we don't allow the range be too close to the bondaries, because as Andrews (1993) pointed out, the power of the test against alternatives with a change point near zero or one is much lower than that of a test against alternatives with changes points anywhere else.

The test results are shown in Table 4.1. We notice that cointegrating value $\boldsymbol{\beta}$ doesn't have

Method	**Statistic**	**Critical Value**		
		Sig=0.01	Sig=0.05	Sig=0.1
$\text{Ave} - \text{LM}_n^{\boldsymbol{\beta}}$	0.7578726	3.37	2.25	1.8
$\text{Exp} - \text{LM}_n^{\boldsymbol{\beta}}$	0.4561919	3.22	2.02	1.53
$\text{Sup} - \text{LM}_n^{\boldsymbol{\beta}}$	2.902988	9.04	10.52	13.92
$\text{Ave} - \text{LM}_n^{\alpha}$	**14.26191**	6.07	4.29	3.54
$\text{Exp} - \text{LM}_n^{\alpha}$	**9.842654**	4.72	3.27	2.64
$\text{Sup} - \text{LM}_n^{\alpha}$	**22.90245**	16.44	12.93	11.2
$\text{Ave} - \text{LM}_n^{\alpha\boldsymbol{\beta}'}$	**15.01978**	7.4	5.59	4.78
$\text{Exp} - \text{LM}_n^{\alpha\boldsymbol{\beta}'}$	**10.46322**	6.01	4.31	3.64
$\text{Sup} - \text{LM}_n^{\alpha\boldsymbol{\beta}'}$	**23.97162**	19.65	15.55	13.8

Table 4.1: LM Test for Structural Change

a structural change during the sample period at all three significant levels, because the test statistics are all smaller than the critical values. The test statistic for adjustment coefficient α are all greater than the critical values, indicating that structural change occurred. Table 4.1 also shows that α and $\boldsymbol{\beta}$ change jointly as well. This is mostly attributed to the structural change of α, as Seo (1998) points out. Since there are more number of coefficients in α than in $\boldsymbol{\beta}$, the critical values of the tests for joint stability is largely depend on those of the stability of α.

Chapter 5

Threshold Vector Error Correction Model

5.1 TVECM model

The structural changes in the long-term equilibrium relationship indicates that VECM model is not adequate. In VECM, the long term equilibrium follows a linear behavior. However, if the structure change exists, the equilibrium should be adjusted to a non-linear behavior. Here we adopt the Threshold Vector Error Correction Model (TVECM).

5.1.1 Introduction of TVECM

In TVECM model, the cointegrating value remains unchanged, while factor changes according to the deviation from the equilibrium. Depending on whether the deviation (or equilibrium error) exceeds a threshold value or not, the VECM model takes different parameters. Usually it is assumed there are one or two threshold values, corsponding to two or three regimes respectively. Take one threshold value for example, the TVECM model can be written as:

$$
\begin{pmatrix} \Delta k_t^{EW} \\ \Delta k_t^{CAN} \end{pmatrix} =
$$

$$
\begin{cases}
c_1 + \alpha_1 \left(k_{t-1}^{EW} - \beta k_{t-1}^{CAN} + w_1 \right) + \sum_{i=1}^{p-1} \Gamma_{1,i} \begin{pmatrix} \Delta k_{t-i}^{EW} \\ \Delta k_{t-i}^{CAN} \end{pmatrix} + \begin{pmatrix} \varepsilon_{1,t}^{EW} \\ \varepsilon_{1,t}^{CAN} \end{pmatrix}, & z_{t-1} > \gamma \\
c_2 + \alpha_2 \left(k_{t-1}^{EW} - \beta k_{t-1}^{CAN} + w_2 \right) + \sum_{i=1}^{p-1} \Gamma_{2,i} \begin{pmatrix} \Delta k_{t-i}^{EW} \\ \Delta k_{t-i}^{CAN} \end{pmatrix} + \begin{pmatrix} \varepsilon_{2,t}^{EW} \\ \varepsilon_{2,t}^{CAN} \end{pmatrix}, & z_{t-1} \leqslant \gamma
\end{cases}
$$

where c_i is the general constant term; w_i is constant term in the long-term equilibrium; α_i is adjustment coefficient; β is cointegrating value; $\Gamma_{n,i}$ are short-term parameters (n is regime number and $i = 1, 2, ..., p-1$) ; z_{t-1} is the deviation from the long-term equilibrium and γ is threshold value.

Which regime the time series is in depends on the value of z_{t-1}. If z_{t-1} is higher than the threshold value γ, then the time series switch to the first regime. If z_{t-1} is lower than γ, it switches to the second regime.

5.1.2 Testing for threshold effect

Before we use the TVECM model, it is important to test whether the non-linear model is superior to a linear model. In other words, we need to test whether the threshold behavior is present in the data set. Balke and Fomby (1997) suggested focusing on the equilibrium error, z_t. They pointed out that if a time series is characterized by threshold co-integration, then z_t will follow a threshold auto-regression (TAR). To test the threshold behavior of z_{t-1}, we adopt the method proposed by Hansen (1999, 1997), because it solved the problem that threshold parameters are not identified under the null hypothesis when testing linearity against threshold alternative. Hansen (1997, 1999) tested TAR(1) against TAR(m) using

sup-F test, where m denotes the number of regimes. The sup-F statistic is calculated as:

$$F_{1m} = n\frac{S_1 - S_m}{S_m},$$

where S_m denotes the sum of squared residuals obtained from least squares estimation. The critical values are determined by bootstrap procedure. Because sup-F tests are affected by the unidentified threshold parameters, the critical values are not fixed. If the sup-F statistic is greater than critical value, then the null hypothesis of TAR(1) is rejected, indicating the data are threshold cointegrated. It can also be used to test 2 regimes against 3 regimes.

5.1.3 Estimating TVECM

Estimating TVECM model usually requires maximum likelihood method using grid search, as proposed by Hansen and Seo (2002). The main idea is that, holding (β, γ) fixed, the likelihood function is only related to β and γ, rather than other parameters. Therefore, building a two dimension grid of (β, γ) will make it possible to find the point which yields the largest likelihood. After finding the β and γ, the parameters can be acquired by OLS. Details of estimation is described below.

The TVECM(2) can be rewritten as:

$$\Delta x_t = A_1^{'} X_{t-1}(\beta) d_{1t}(\beta, \gamma) + A_1^{'} X_{t-1}(\beta) d_{2t}(\beta, \gamma) + \varepsilon_t, \tag{5.1}$$

where A is coefficients matrix; $X_{t-1}(\beta) = (1, z_{t-1}(\beta), \Delta X_{t-1})^{'}$ and $x_t = (k_t^{EW}, k_t^{CAN})^{'}$, $z_{t-1}(\beta) = k_t^{EW} - \beta k_t^{CAN}$; $d_{1t}(\beta, \gamma) = 1(z_{t-1}(\beta) \leqslant \gamma)$ and $1(\cdot)$ denotes the indicator function; $d_{2t}(\beta, \gamma) = 1(z_{t-1}(\beta) > \gamma)$ and Σ is the covariance matrix.

Under the assumption that the errors ε_t are iid Gaussian, the Gaussian likelihood of TVECM(2) is:

$$L_n(A_1, A_2, \Sigma, \beta, \gamma) = -\frac{n}{2} log|\Sigma| - \frac{1}{2}\sum_{t=1}^{n} \varepsilon_t(A_1, A_2, \beta, \gamma)^{'} \Sigma^{-1} (\varepsilon_t, A_1, A_2, \beta, \gamma). \tag{5.2}$$

Holding (β, γ) fixed, estimation for (A_1, A_2, Σ) is simply ordinary least square (OLS) regression of ΔX_t on $X_{t-1}(\beta)$ for the subsamples in each regime. The likelihood function can be simplified to:

$$\begin{aligned} \mathrm{L}_n(\beta, \gamma) &= \mathrm{L}_n(\hat{A}_1, \hat{A}_2, \hat{\Sigma}, \beta, \gamma) \\ &= -\frac{n}{2}\log|\hat{\Sigma}(\beta, \gamma)| - \frac{np}{2}, \end{aligned} \tag{5.3}$$

which is only related to (β, γ). If we have the value of (β, γ), the coefficients matrix can be calculated easily.

To find out which pair of $(\hat{\beta}, \hat{\gamma})$ yields the lowest $\log|\hat{\Sigma}(\beta, \gamma)|$, Hansen and Seo (2002) suggested using a grid search over the two-dimensional space for (β, γ). γ is searched over a evenly spaced grid which contain 90% of z_{t-1}. Andrews (1993) suggested using 70% $\sim$ 90% of z_{t-1}. β is searched over a evenly spaced grid which is a large confidence interval for β constructed from linear VECM estimate. In practice, however, experiences show the confidence interval are small for the cointegrating values no matter how large it is. So it is recommended to inspect the plot of the grid search (Stigler, 2010).

5.2 Numerical Results

Using Hansen's testing method, Table 5.1 shows the results for our data set. It is shown that linearity is strongly rejected at 1% significant level, when testing linearity against two regimes. It is also rejected when testing against three regimes at 0.05 significant level, but not at 1% significant level. In addition, when testing the two regimes against three regimes, we can not reject two regimes at all three significant levels. We conclude that our data has threshold effect and two regimes TVECM model seems to be sufficient.

We fit the data set into TVECM(2) model, and the estimated model is shown below.

Regime	Test statistic	Critical Value		
		Sig=0.1	Si=0.05	Sig=0.01
1 vs 2	**17.34656**	9.887284	11.74917	16.72401
1 vs 3	**19.04931**	17.265308	19.00977	25.09488
2 vs 3	1.416951	8.98552	11.25023	15.48487

Table 5.1: Hansen's Linearity Test Results

$$\begin{pmatrix} \Delta k_t^{EW} \\ \Delta k_t^{CAN} \end{pmatrix} = \begin{pmatrix} -1.4552 \\ -0.6877 \end{pmatrix} + \begin{pmatrix} -0.4883 \\ 0.0296 \end{pmatrix}\left(k_{t-1}^{EW} - 0.9917k_{t-1}^{CAN} - 1.0298\right)$$
$$+ \begin{pmatrix} -0.4656 & 0.3396 \\ -0.0207 & -0.0486 \end{pmatrix}\begin{pmatrix} \Delta k_{t-1}^{EW} \\ \Delta k_{t-1}^{CAN} \end{pmatrix} + \begin{pmatrix} -0.8236 & -0.3108 \\ -0.1349 & -0.1925 \end{pmatrix}\begin{pmatrix} \Delta k_{t-2}^{EW} \\ \Delta k_{t-2}^{CAN} \end{pmatrix}$$
$$+ \begin{pmatrix} -0.5074 & 0.078 \\ -0.0711 & 0.2052 \end{pmatrix}\begin{pmatrix} \Delta k_{t-3}^{EW} \\ \Delta k_{t-3}^{CAN} \end{pmatrix} + \begin{pmatrix} \varepsilon_t^{EW} \\ \varepsilon_t^{CAN} \end{pmatrix}, \qquad z_{t-1} > -0.1132 \tag{5.4}$$

$$\begin{pmatrix} \Delta k_t^{EW} \\ \Delta k_t^{CAN} \end{pmatrix} = \begin{pmatrix} 0.0189 \\ -0.0289 \end{pmatrix} + \begin{pmatrix} -0.1885 \\ 0.0981 \end{pmatrix}\left(k_{t-1}^{EW} - 0.9917k_{t-1}^{CAN} - 0.5167\right)$$
$$+ \begin{pmatrix} -0.2404 & 0.4099 \\ -0.0194 & 0.1105 \end{pmatrix}\begin{pmatrix} \Delta k_{t-1}^{EW} \\ \Delta k_{t-1}^{CAN} \end{pmatrix} + \begin{pmatrix} 0.2771 & 0.1222 \\ 0.0968 & 0.1481 \end{pmatrix}\begin{pmatrix} \Delta k_{t-2}^{EW} \\ \Delta k_{t-2}^{CAN} \end{pmatrix}$$
$$+ \begin{pmatrix} 0.0323 & 0.7685 \\ 0.1537 & -0.0212 \end{pmatrix}\begin{pmatrix} \Delta k_{t-3}^{EW} \\ \Delta k_{t-3}^{CAN} \end{pmatrix} + \begin{pmatrix} \varepsilon_t^{EW} \\ \varepsilon_t^{CAN} \end{pmatrix}, \qquad z_{t-1} < -0.1132 \tag{5.5}$$

where the estimated variance-covariance equal to $\begin{bmatrix} 1.0956 & 0.3053 \\ 0.3053 & 0.3550 \end{bmatrix}$.

As we can see from the model, the threshold value is estimated to be -0.1132. If the deviation is higher than -0.1132, the long term equilibrium is $k_t^{EW} = 0.9917k_t^{CAN} + 1.0298$,

the corresponding adjustment coefficient is $\begin{pmatrix} -0.4883 \\ 0.0296 \end{pmatrix}$. If the deviation is below -0.1132, the long term equilibrium is $k_t^{EW} = 0.9917 k_t^{CAN} + 0.5167$, and the corresponding adjustment coefficient is $\begin{pmatrix} -0.1885 \\ 0.0981 \end{pmatrix}$. From equation (5.4) and equation (5.5), we also see that the adjustment for k_t^{EW} and k_t^{CAN} are towards opposite directions in both regimes, since the adjustment coefficient is negative for k_t^{EW} and positive for k_t^{CAN}.

When the deviation is higher than 0, k_{t-1}^{EW} is much larger than k_{t-1}^{CAN}. Multiplying by the negative coefficient -0.4883 results into a negative correlation to Δk_t^{EW} and thus pulls down k_t^{EW}. On the other hand, multiplying the deviation by the positive coefficient 0.0296 results into a positive correlation to Δk_t^{CAN} and hence pulls up k_t^{CAN}. This adjustment reduces the gap between k_t^{EW} and k_t^{CAN}, consequently pulls them back towards the long term equilibrium. When the deviation is in between -0.1132 and 0, the process is again in the first regime. The deviation is multiplied by -0.4883 and 0.0296 for EW and CAN, respectively. The error correction term will enlarge the deviation temporarily. Once the deviation exceeds 0, the error correction term will pull the two processes towards their long-term equilibrium. Another case is when the the deviation is lower than the threshold value, or the deviation is a negative number indicating k_{t-1}^{EW} is much smaller than k_{t-1}^{CAN}. Then the negative deviation multiplied by -0.1885 results into a positive Δk_t^{EW}, while multiplied by 0.0981 gives a negative Δk_t^{CAN}. The adjustment coefficient pulls up k_t^{EW} and pulls down k_t^{CAN} as a result, so the difference between k_t^{EW} and k_t^{CAN} was also reduced.

Figure 5.1 shows how the deviation changes the regime. The picture shows that during 1925 to 1940 and 1970 to 1995, the deviation is positive and most are adjusted by the long term equilibrium relationship in the upper regime. During the year of 1940 to 1970 and 1995 to 2011, the deviation is negative and most are adjusted by the long term equilibrium relationship in the down regime. But the deviations all fluctuate around the threshold value which is very close to 0.

Moreover, we also notice that the cointegrating value is 0.9917 in TVECM model under

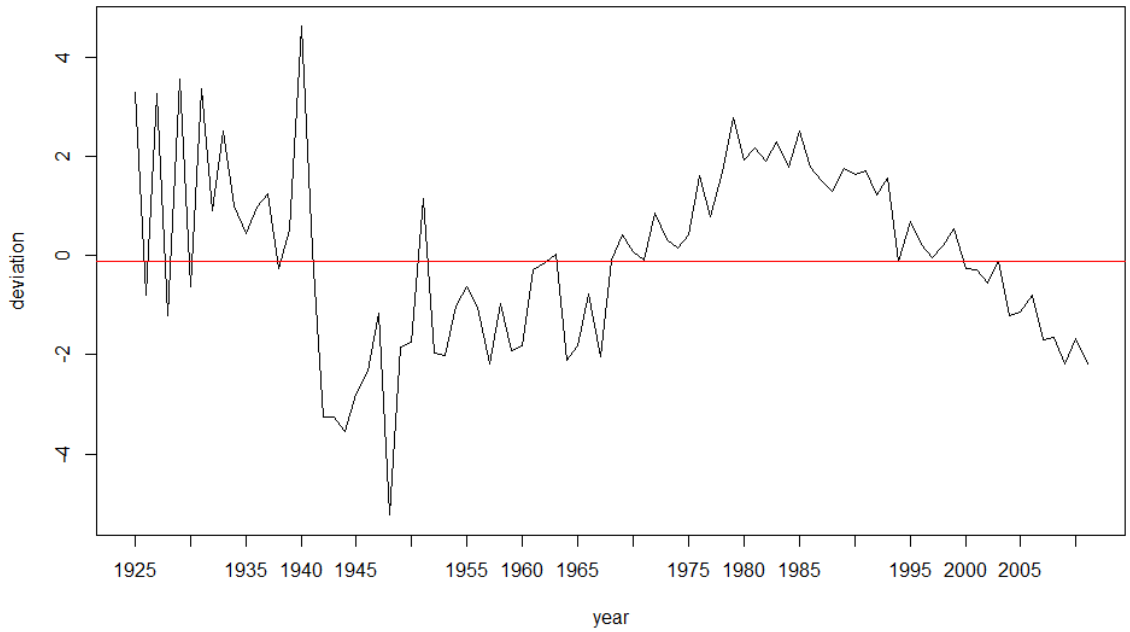

Figure 5.1: Deviation in different regimes by TVECM

both regimes, which is very close to the 0.992 in VECM model. Considering in chapter 4 when testing the structural change of VECM model, we find the cointegration value β doesn't have a structure change. So this estimated cointegration value in TVECM model matches well with the structural change test.

5.3 Model parsimonious and diagnostic checking

Furthermore, model parsimonious and diagnostic checking are also performed. For model parsimony, we use Bayesian Information Criteria (BIC) to compare TVECM(2) and TVECM(3). The result is shown in Table 5.2. TVECM(2) has a lower BIC value, which means it provides better goodness of fit than TVECM(3).

For diagnostic checking, we examine the autocorrelation and the normality of the residuals from TVECM(2). Table 5.3 shows the testing results of autocorrelation. The p-values for

	TVECM(2)	TVECM(3)
BIC	698.14	828.25

Table 5.2: Results of Model Parsimonious Using BIC

Lag	Statistic	p-value
1	3.76	0.48
2	6.72	0.52
3	8.07	0.68
4	11.61	0.63
5	14.22	0.65
6	17.04	0.67
7	19.88	0.67
8	23.23	0.65
9	26.34	0.65
10	28.93	0.67

Table 5.3: Autocorrelation Check of Residuals in TVECM(2)

lag order 1 to 10 are all large, indicating there is no autocorrelation in the residuals.

We perform three normality tests: Mardia's Test for skewness, Mardia's Test for kurtosis and Henze-Zirkler Test. Test results are shown in Table 5.3. Since all p-values are large , we can't reject the null hypothesis that the residuals are normality distributed.

	Test statistic	p-value
Mardia's Test (skew)	3.387762	0.4951482
Mardia's Test (kurtosis)	1.135402	0.2562069
Henze-Zirkler Test	0.5548691	0.4409921

Table 5.4: Normality Check of Residuals in TVECM(2)

5.4 Forecasting Performance

We use Monto Carlo simulation to forecast future mortality rates. We forecast k_t^{EW} and k_t^{CAN} from year 2012 to 2031 based on the estimated TVECM(2) model, and also determine the 95% prediction interval. The simulation procedures are shown as follows:

(1) Simulate 5000 bivariate normal random vector for the error term. The bivariate

normal distribution has mean equal to 0 and variance-covariance matrix as estimated for the TVECM(2) model.

(2) Determine simulated k_t^{EW} and k_t^{CAN} using the simulated errors for $t = 2012$.

(3) Repeat step (1) and (2) for $t = 2013, 2014, \ldots, 2031$.

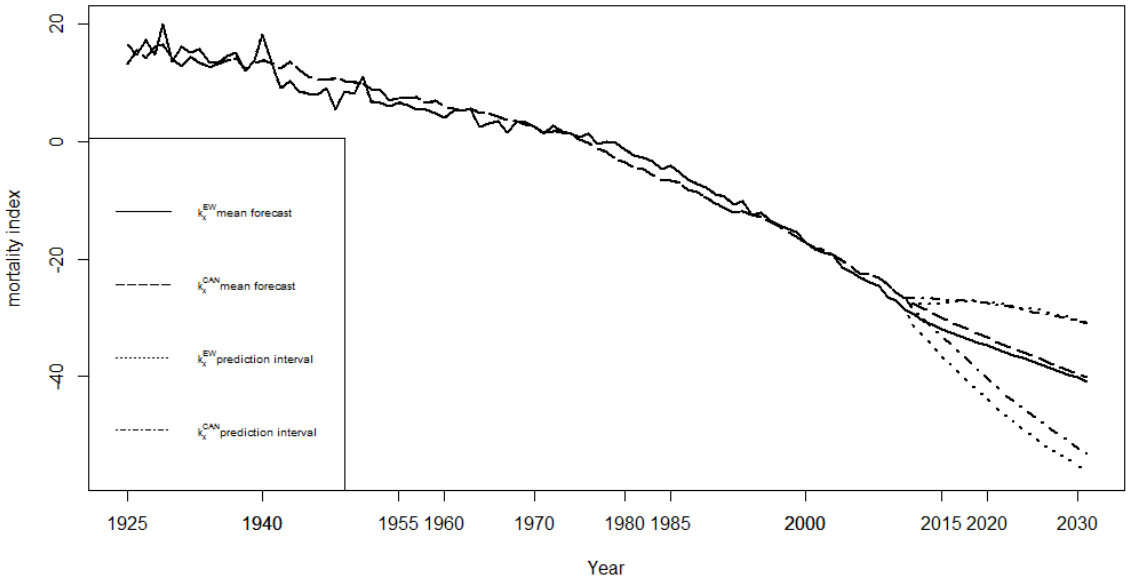

Figure 5.2: Forecasts of k_t^{EW} and k_t^{CAN} using TVECM(2) model

Figure 5.2 shows the mean prediction and 95% prediction interval for k_t^{EW} and k_t^{CAN}. 95% prediction interval is determined by the 2.5% and 97.5% percentile of the simulated values. It shows that both simulated k_t^{EW} and k_t^{CAN} have a downward trend in the following 20 years, and k_t^{CAN} is slightly higher than k_t^{EW}. The gap between k_t^{EW} and k_t^{CAN} is large in the first few years. However, it shrinks in the later years. The prediction interval of k_t^{EW} is larger than that of k_t^{CAN}. That is because k_t^{EW} has more fluctuation than k_t^{CAN} historically as we mentioned before.

Figure 5.3 and Figure 5.4 compare the forecasts from VECM and TVECM(2) for k_t^{EW} and k_t^{CAN}, respectively. For both k_t^{EW} and k_t^{CAN}, VECM mean forecasts are higher than TVECM(2) mean forecasts and the gap becomes larger with forecasting period. This indicates

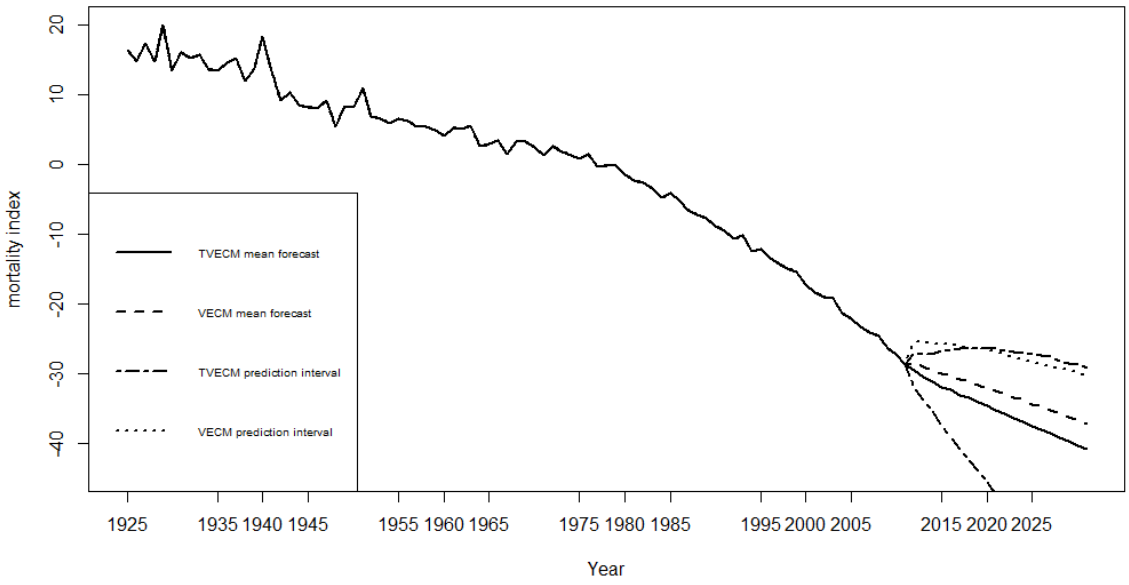

Figure 5.3: Comparison of forecasts of k_t^{EW} using VECM and TVECM

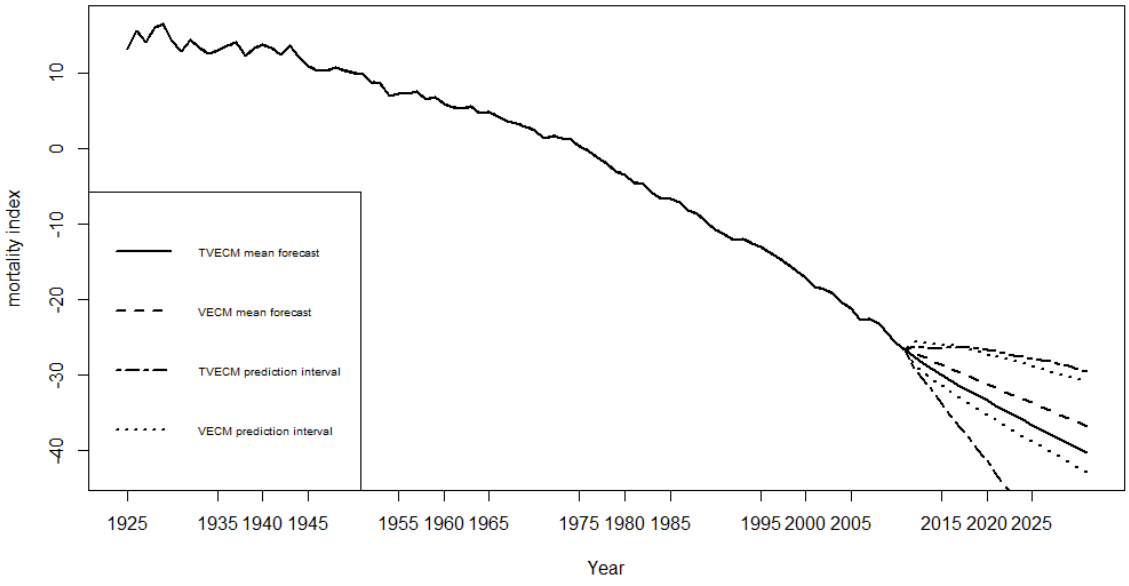

Figure 5.4: Comparison of forecasts of k_t^{CAN} using VECM and TVECM

the resulted mortality rates forecasts by VECM will be higher than by TVECM. Moreover, the prediction interval under TVECM is larger than VECM. That is because TVECM switches regimes, thereby leading to higher variance of predictions. Therefore, without considering possible changes in the long-term equilibrium, we will underestimate longevity risk.

Chapter 6

Pricing Longevity Bonds

In this chapter, we apply the TVECM model to longevity bond pricing using risk-neutral method. First, we introduce the structure of Kortis bond. Second, we show details about the risk-neutral pricing method. Finally, we summeriza the numerical result of bond pricing.

6.1 Kortis Bond

Kortis Bond, issued by Swiss Re in December 2010, is designed to hedge the mismatch between Swiss Re's annuity portfolio in the UK and insurance portfolio in the US. Swiss Re has reinsuring life insurance policies in the US and annuity policies in the UK. Generally, these two portfolios are natural hedges of each other (Cox and Lin, 2007), since mortality improvement leads to less benefit payouts for life insurances but more for annuities. However, natural hedges is not always perfect, due to the existence of basis risk. Basis risk is almost unavoidable due to two main reasons (Hunt and Blake, 2015):

(1) Different lifestyles and medical systems in the US and UK result in different trends in mortality;

(2) Annuity holders are usually older than life insurance holders.

Therefore, Kortis Bond was launched to hedge this mismatch. When the mortality im-

provement in UK is much higher than that in US, the principal repayment of the bond will be reduced, offsetting the higher annuity benefit payouts faced by Swiss Re. For bond investors, this bond pays quarterly coupons at a floating rate of 5.0% above LIBOR with a return of principal at maturity in January 2017 (extendable until July 2019). The principal is linked to an index called Longevity Divergence Index Value (LDIV), which measurs the divergence between the mortality rates of UK and the US.

In this thesis, we price an illustrative bond with the same structure but different population data. This bond is issued at the end of year 2011 and will mature at the end of year 2019. In addition, we assume the issuer has annuity policies in England and Wales and life insurance business in Canada. The goal of this bond is to headge the part of longevity risk in EW annuities that cannot be fully hedged by the life insurance policies in Canada. The LDIV is calculated in three steps:

Step 1: Calculate observed improvement for each age:

$$\text{Improvement}_n(x,t)^p = 1 - \left[\frac{m^p_{x,t}}{m^p_{x,t-n}}\right]^{\frac{1}{n}}, \tag{6.1}$$

where p is EW or CAN; n is term of the bond. Here $n = 8$ and $t = 2019$. From the equation (6.1), we can see if $m^p_{x,t}$ is larger than $m^p_{x,t-n}$, the improvement is negative, indicating mortality deterioration.

Step 2: Calculate improvement index for each country:

$$\text{Index}_{(t,p)} = \frac{1}{1 + x_2 - x_1} \sum_{x=x_1}^{x_2} \text{Improvement}^p_8(x,t). \tag{6.2}$$

This index represents the average improvement rate observed across ages x_1 to x_2 over the eight years for t population p. We use age 75 to 85 for EW and age 55 to 65 for CAN.

Step 3: Calculate the LDIV:

$$\text{LDIV}(2019) = \text{Index}_{(2019,EW)} - \text{Index}_{(2019,CAN)}. \tag{6.3}$$

The principal of the bond is reduced by a "principal reduction factor" (PRF) given by:

$$PRF = \max\left(\min\left(\frac{LDIV(2019) - \text{ap}}{\text{ap} - \text{ep}}, 1\right), 0\right), \tag{6.4}$$

where ap is the point of attachment and ep is the point of exhaustion. From equation (6.4), we can see there are generally three scenarios of the principal repayment:

Scenario 1: $LDIV(2019) < \text{ap}$ and $PRF = 0$. It means the divergence of mortality improvements between EW and CAN is small, hence the longevity risk exposure is moderate. Full principal will be returned to the bond investors.

Scenario 2: $\text{ap} < LDIV(2019) < \text{ep}$ and $PRF = \frac{LDIV(2019)-\text{ap}}{\text{ap}-\text{ep}}$. Under this condition, the insurance company has stress on annuity book, due to the large divergence of mortality improvements between EW and CAN. However, the principal of the bond is reduced to compensate the loss on annuity book.

Scenario 3: $LDIV(2019) > \text{ep}$ and $PRF = 1$. In this scenario, the divergence of mortality improvemetns between EW and CAN is very large , the loss on the annuity book is very high. The principal of the bond is 100% reduced to relieve the huge financial burden of the insurance company.

6.2 Risk-Neutral Method

A common method to price financial securities is to use risk-neutral measures. A risk-neutral investor is indifferent with a riskless asset and a risky bet with an expected payoff equals to the riskless asset. The probabilities of the bet's price up and down in the risk-neutral world is called risk-neutral probabilities. However, these probabilities are usually not the same with real world probabilities. How to convert the real world probabilities to risk-neutral probabilities is the core issue in risk-neutral pricing. Several researchers (Cox et al., 2006; Wang, 2007; Yang and Wang, 2013) have applied Wang transform to transform real world probabilities to risk-neutral probabilities and pricing mortality-linked securities.

In this paper, we follow Yang and Wang (2013) and apply multivariate Wang transform to the TVECM model, to calculate the risk-neutral mortality rates and finally price the bond.

To obtain the mortality rates under risk-neutral measure, we start from the error term in TVECM model. Since the error term follows normal distribution, it will still be normally distributed after the multivariate Wang transform. Let $\tilde{\varepsilon_t}$ denote the error term in TVECM under risk-neutral measure. Using the multivariate Wang transform, we have:

$$\tilde{\varepsilon}_t^{EW} = \varepsilon_t^{EW} + \lambda_\varepsilon^{EW} v_{EW,EW} + \lambda_\varepsilon^{CAN} v_{EW,CAN}, \tag{6.5}$$

$$\tilde{\varepsilon}_t^{CAN} = \varepsilon_t^{CAN} + \lambda_\varepsilon^{EW} v_{CAN,EW} + \lambda_\varepsilon^{CAN} v_{CAN,CAN}, \tag{6.6}$$

where λ_ε^{EW} and $\lambda_\varepsilon^{CAN}$ are the risk adjustment parameter for the mortality index; $v_{i,j}$ is the covariance between ε_t^i and ε_t^j, where i and j represent countries. After the transform, the mean of $\tilde{\varepsilon}_t$ becomes $\lambda_\varepsilon^{EW} v_{EW,EW} + \lambda_\varepsilon^{CAN} v_{EW,CAN}, \quad \lambda_\varepsilon^{EW} v_{CAN,EW} + \lambda_\varepsilon^{CAN} v_{CAN,CAN}$, and the variance remains the same with ε_t, since adding a constant does not change the variance. Based on $\tilde{\varepsilon}_t^{EW}$ and $\tilde{\varepsilon}_t^{CAN}$, we can calculate the $\tilde{k}_t^{EW}$ and $\tilde{k}_t^{CAN}$.

Using the same idea, we transform the error terms in Lee-Carter model. The risk-neutral error terms are denoted by $\Delta\tilde{e}_{x,t}$, and expressed as follows:

$$\Delta\tilde{e}_{x,t}^{EW} = \Delta e_{x,t}^{EW} + \sum_{y=75}^{85} \lambda_y^{EW} \sigma_{x,y}^{EW,EW} + \sum_{y=55}^{65} \lambda_y^{CAN} \sigma_{x,y}^{EW,CAN}, \tag{6.7}$$

$$\Delta\tilde{e}_{x,t}^{CAN} = \Delta e_{x,t}^{CAN} + \sum_{y=75}^{85} \lambda_y^{EW} \sigma_{x,y}^{CAN,EW} + \sum_{y=55}^{65} \lambda_y^{CAN}, \sigma_{x,y}^{CAN,CAN} \tag{6.8}$$

where λ_y^{EW} and λ_y^{CAN} are risk adjustment parameters for $\Delta e_{y,t}^{EW}$ and $\Delta e_{y,t}^{EW}$, respectively. $\sigma_{x,y}^{i,j}$ denotes the age-specific covariance between $\Delta e_{x,t}^i$ and $\Delta e_{y,t}^j$, where i and j represent country.

Based on the Lee-Carter model, the risk-neutral mortality difference between year 2019

and year 2011 can be expressed as:

$$\ln(\tilde{m}_{x,2019}) - \ln(\tilde{m}_{x,2011}) = a_x + b_x\tilde{k}_{2019} + \tilde{e}_{x,2019} - a_x - b_x k_{2011} - \tilde{e}_{x,2011}. \tag{6.9}$$

Since the mortality rates in 2011 are known, $\tilde{m}_{x,2011} = m_{x,2011}$ and $\tilde{e}_{x,2011} = e_{x,2011}$. Therefore, we have:

$$\ln(\tilde{m}_{x,2019}) = \ln(m_{x,2011}) + b_x(\tilde{k}_{2019} - k_{2011}) + (\Delta\tilde{e}_{x,2012} + ... + \Delta\tilde{e}_{x,2019}). \tag{6.10}$$

Risk-neutral LDIV and PRF are calculated using these simulated risk-neutral mortality rates.

6.3 Pricing formula

Figure 6.1 illustrates the payoff structure of the bond. Note that i denotes 3-month LIBOR and x denotes the spread over LIBOR. The longevity bond is traded at its face value. When the bond matures, the principal will be returned but may be subject to erosion. The bond holder receives a quarterly coupon greater than LIBOR to compensate the possibility of principal erosion. The spread over LIBOR is the "price" we need to determine. In the original Kortis bond, the spread is 5% over 3-month LIBOR, although some researchers find it too high (Chen et al.).

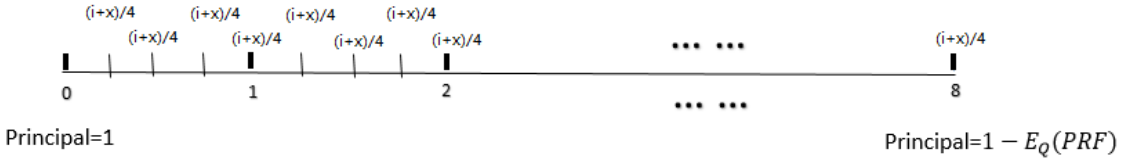

Figure 6.1: Structure of longevity bond

Under the risk-neutral world, we have:

$$1 = \sum_{n=\frac{1}{4},\frac{2}{4},\ldots,8} e^{-nr_n}\left(\frac{i+x}{4}\right) + [1 - E_Q(PRF)]e^{-8r_8}, \tag{6.11}$$

where r_n is the yield rate of a n-year US treasury bond. $E_Q(PRF)$ is the expectation of PRF under risk-neutral measure. Since r_n and i are known, this equation can be easily solved after obtaining $E_Q(PRF)$.

6.4 Numerical Results

We use the Monto Carlo simulation to calculate $E_Q(PRF)$. In the simulation, there are two assumptions:

(1) we assume all the risk adjustment parameters take the same value. We demonstrate the pricing results using the value of -0.1, -0.3 and -0.5. Cox et al. (2006) found the market price of risk is 0.1792 for male annuitants and 0.2312 for female annuitants in pricing survivor derivatives. Lin and Cox (2008) found that the market price of risk for EIB bond is 0.2408. Therefore we would like to set the value of λ to be around. In our case, negative market price of risk is reasonable.

(2) The 3-month LIBOR is set to 0.6%.

Based on the assumptions, we simulate 5000 mortality rate paths for each age group, calculate corresonding $\widetilde{LDIV}$ and $\widetilde{PRF}$, and finally determine the spread over LIBOR based on the pricing formula.

6.4.1 Simulating risk-neutral mortality rates

First, we use the following proceddures to simulate $\tilde{k}_t^{EW}$ and $\tilde{k}_t^{CAN}$.

(1) Generate 5000 error terms from bivariate normal distribution with mean equal to $(\lambda_\varepsilon^{EW} v_{EW,EW} + \lambda_\varepsilon^{CAN} v_{EW,CAN}, \lambda_\varepsilon^{EW} v_{CAN,EW} + \lambda_\varepsilon^{CAN} v_{CAN,CAN})'$, and variance-covariance

matrix equal to $\begin{bmatrix} 1.0956 & 0.3053 \\ 0.3053 & 0.3550 \end{bmatrix}$.

(2) Calculating $\tilde{k}_t^{EW}$ and $\tilde{k}_t^{CAN}$ for $t = 2012$ using TVECM model based on the simulated error vectors.

(3) Repeat step (1) and (2) for $t = 2013, 2014, ..., 2019$.

Figure 6.2 shows the forecasts of $\tilde{k}_t^{EW}$ and $\tilde{k}_t^{CAN}$ from year 2012 to 2031 with market price of risk set to -0.1.

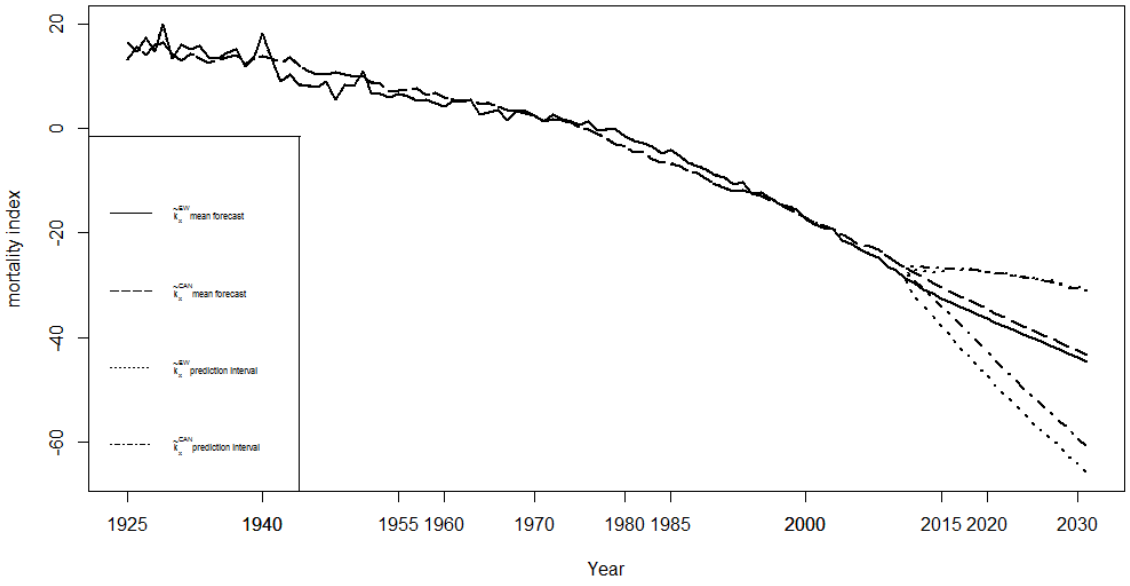

Figure 6.2: Simulated $\tilde{k}_t^{EW}$ and $\tilde{k}_t^{CAN}$ with $\lambda_\varepsilon^{EW} = \lambda_\varepsilon^{CAN} = -0.1$

Second, we simulate $\Delta\tilde{e}_{x,t}^{EW}$ and $\Delta\tilde{e}_{x,t}^{CAN}$ in Lee-Carter model where $x \in [75, 85]$ for EW and $x \in [55, 65]$ for CAN. Using multivariate normal distrbubtion, $\Delta\tilde{e}_{2019}$ is the summation of $\Delta\tilde{e}_{x,2012}^{i} + \Delta\tilde{e}_{x,2013}^{i} + ... + \Delta\tilde{e}_{x,2019}^{i}$ where i denotes country.

Finally, we calculate $\tilde{m}_{x,2019}^{EW}$ and $\tilde{m}_{x,2019}^{CAN}$ using simulated $\tilde{k}_{2019}^{EW}$, $\tilde{k}_{2019}^{CAN}$, $\tilde{e}_{x,2019}^{EW}$ and $\tilde{e}_{x,2019}^{CAN}$.

6.4.2 LDIV and PRF

Same with the Kortis bond, we set the "point of attachment" and "point of exhausted" at the 94.69% and 98.19% percentile of the LDIV, respectively. Figure 6.3 shows the simulated LDIVs. The upper horizontal line represents the 98.19% quantile of the simulated values; the middle line represents the 94.69% quantile; and the lower line is the minimum value of the simulated LDIV. The "point of attachment" is 0.065% and the "point of exhausted" is 0.237%.

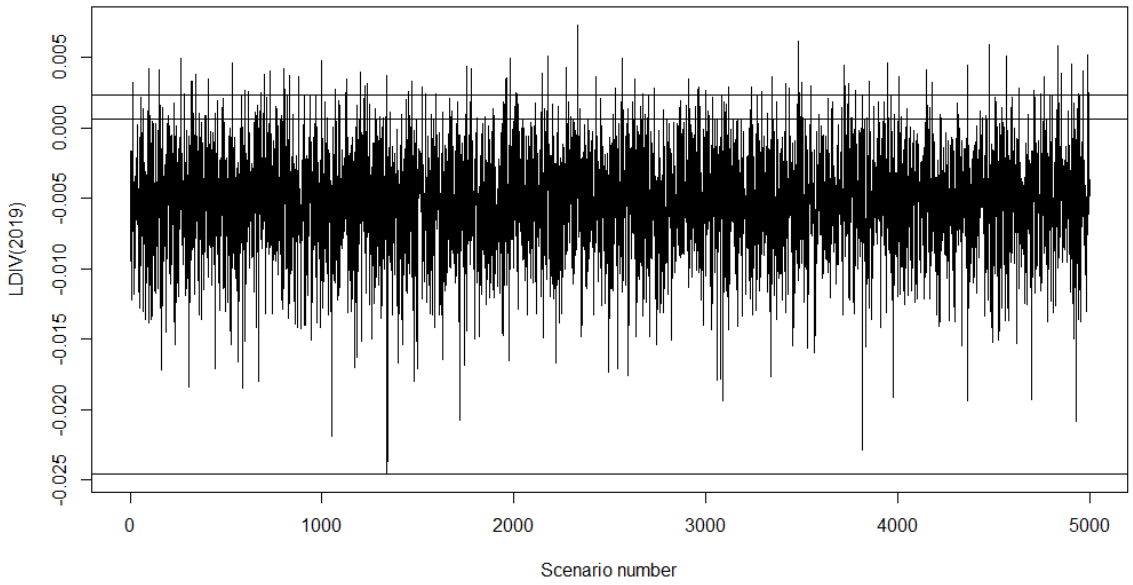

Figure 6.3: Simulated LDIV(2019)

Denote LDIV(2019) under risk-neutral measure as $\widetilde{LDIV}(2019)$. To calculate $E_Q(PRF)$, we first obtain simulated $\widetilde{LDIV}(2019)$ based on the simulated $\tilde{m}_{x,2019}$. With "point of attachment"=0.065% and "point of exhausted"=0.237%, PRF under risk-neutral measure can also be calculated. $E_Q(PRF)$ is then calculated by taking the average of the simulated risk-neutral PRF's.

When the market price of risk is -0.1, we find $E_Q(PRF) = 0.045623$ and the resulting spread over LIBOR is 3.248%. Table 6.1 shows the value of $E_Q(PRF)$ and spread over

		$\mathbf{E_Q(PRF)}$	**Spread over LIBOR**
TVECM	$\lambda = 0$	0.027025	3.0576%
	$\lambda = -0.1$	0.045623	3.248%
	$\lambda = -0.3$	0.119027	3.99949%
	$\lambda = -0.5$	0.252993	5.371%
VECM	$\lambda = 0$	0.128121	4.0926%
	$\lambda = -0.1$	0.141347	4.228%
	$\lambda = -0.3$	0.229589	5.1314%
	$\lambda = -0.5$	0.376751	6.638%

Table 6.1: $E_Q(PRF)$ and spread over LIBOR using different market price of risk

LIBOR using different market price of risk.

As we can see from Table 6.1, the coupon rate increases with market price of risk, and TVECM yields a lower coupon rate than VECM. Although mortality rate forecasts are lower using TVECM for both EW and CAN than using VECM, the difference between the mortality improvement of the two populations actually shrinks. Therefore, the LDIV using TVECM is smaller, thereby resulting in lower price of risk.

6.4.3 Calibrating market price of risk

In the earlier studies, we set the market price of risk to be -0.1, -0.3 and -0.5 and calculate the spread over LIBOR. In this section, we solve for the values of market price of risk when fixing the spread over LIBOR to various values. In addition, we make a comparison between TVECM results and VECM results. In order to control the external variable, we use the same random standard normal distributed seeds for simulating error terms in TVECM and VECM.

The following procedures are used:

(1) Simulate 5000 standard bivariate normal error terms.

(2) Linearly transform the simulated standard normal vectors such that its mean equal to $(\lambda_\varepsilon^{EW} v_{EW,EW} + \lambda_\varepsilon^{CAN} v_{EW,CAN}, \lambda_\varepsilon^{EW} v_{CAN,EW} + \lambda_\varepsilon^{CAN} v_{CAN,CAN})'$ and variance-covariance matrix equal to that of the residuals from TVECM model. These new error terms are the simulated risk-neutral error terms for TVECM model.

(3) Linearly transform the simulated standard normal vectors such that its mean equal to $(\lambda_{\varepsilon}^{EW} v_{EW,EW} + \lambda_{\varepsilon}^{CAN} v_{EW,CAN}, \lambda_{\varepsilon}^{EW} v_{CAN,EW} + \lambda_{\varepsilon}^{CAN} v_{CAN,CAN})'$ and variance-covariance matrix equal to that of the residuals from VECM model. These new error terms are the simulated risk-neutral error terms for VECM model.

(4) Calculated simulated $\tilde{k}_{2019}$, $\tilde{m}_{x,2019}$, $\widetilde{LDIV}(2019)$ and $\widetilde{PRF}$ as described earlier with unknown market price of risk under both TVECM and VECM model.

(5) Solve for the market price of risk using iterative algorithms.

Based on these procedures, Table 6.2 shows the market price of risk under different scenarios:

Spread over LIBOR		4.5%	5.0%	5.5%
Market price of risk	**TVECM**	-0.3873	-0.457	-0.5149
	VECM	-0.1047	-0.213	-0.3063

Table 6.2: Market price of risk under different spread over LIBOR

As we can see from Table 6.2, the absolute value of the market price of risk increases with the spread over LIBOR for both TVECM and VECM. Higher market price of risk means bond investors require a higher return, and hence a higher coupon rate.

The Kortis bond was issued with a spread of 5% over 3-month LIBOR. In our case, 5% spread corresponds to the market price of risk of -0.457 for TVECM and -0.213 for VECM. The large difference between the two indicates that the incorporation of changes in long-term equilibrium has a profound impact on the pricing of the longevity bond.

Chapter 7

Conclusion

In this thesis, we test the long-term equilibrium between the mortality rates of England and Wales and Canada. We then apply our results in pricing a longevity bond. Specifically, we first fit the Lee-Carter model to EW and CAN mortality rates using SVD method and obtain the mortality indexes. We use the data for age 50 to 89 from year 1925 to 2011. We find a downward trend in both regions' mortality indexes. We also observe that the EW mortality index fluctuates more than CAN mortality index.

Our test shows that there exists a long-term equilibrium between k_t^{EW} and k_t^{CAN}. Therefore, we use VECM model to capture this equilibrium. The error correction term includes an adjustment coefficient and the equilibrium relation. By applying structural change test, we find that the adjustment coefficient α changes during the sample time period, while the equilibrium relation does not change. Therefore, VECM is not suitable for our data.

We further consider TVECM model to adjust the long-term equilibrium relationship. In the TVECM, the long-term relation switches regimes based on the value of the threshold variable. Our test results show that two regimes are reasonable. When comparing the forecasts of mortality index between TVECM and VECM, we find the TVECM gives a lower mortality index, thereby indicating higher longevity risk.

Finally, we price an 8-year longevity bond that hedges the mismatch between annuity

book and insurance portfolio for an insurance company. Our numerical results show that TVECM model indicates a higher market premium of risk than VECM when the coupon rate of the bond is fixed.

Therefore, incorporating possible changes in the long-term equilibrium has a significant impact on the pricing of longevity bond.

Appendix A

Derivation of VECM model

In VAR model, the $t \times 1$ vector X_t with lag order p can be expressed as:

$$\begin{aligned}
X_t &= c + \Phi_1 X_{t-1} + \Phi_2 X_{t-2} + \Phi_3 X_{t-3} + ... + \Phi_p X_{t-p} + \varepsilon_t \\
&= c + \Phi_1 X_{t-1} + \Phi_2 (X_{t-1} - \Delta X_{t-1}) + \Phi_3 (X - t - 1 - \Delta X_{t-1} - \Delta X_{t-2}) + ... \\
&+ \Phi_p (X - t - 1 - \Delta X_{t-1} - \Delta X_{t-2} - ... - \Delta X_{t-p+1} + \varepsilon_t \\
&= c + (\Phi_1 + \Phi_2 + \Phi_3 + ... + \Phi_p) X_{t-1} - (\Phi_2 + \Phi_3 + ... + \Phi_p) \Delta X_{t-1} - (\Phi_3 + ... + \Phi_p) \Delta X_{t-2} \\
&- ... - \Phi_p \Delta X_{t-p+1} + \varepsilon_t
\end{aligned} \tag{A.1}$$

Subtracting X_{t-1} on both side of the equation, we have:

$$\begin{aligned}
\Delta X_t = c &+ (\Phi_1 + \Phi_2 + \Phi_3 + ... + \Phi_p - I) X_{t-1} - (\Phi_2 + \Phi_3 + ... + \Phi_p) \Delta X_{t-1} \\
&- (\Phi_3 + ... + \Phi_p) \Delta X_{t-2} - ... - \Phi_p \Delta X_{t-p+1} + \varepsilon_t
\end{aligned} \tag{A.2}$$

Let $\Pi = \Phi_1 + \Phi_2 + \Phi_3 + ... + \Phi_p - I$ and $\Gamma_i = \Phi_{i+1} + \Phi_{i+2} + ... + \Phi_p$, we obtain the VECM form:

$$\Delta X_t = c + \Pi X_{t-1} - \sum_{i=1}^{p-1} \Gamma_i \Delta X_{t-i} + \varepsilon_t \tag{A.3}$$

In our case, we have

$$\begin{pmatrix} \Delta k_t^{EW} \\ \Delta k_t^{CAN} \end{pmatrix} = c + \Pi \begin{pmatrix} k_{t-1}^{EW} \\ k_{t-1}^{CAN} \end{pmatrix} + \sum_{i=1}^{p-1} \Gamma_i \begin{pmatrix} \Delta k_{t-i}^{EW} \\ \Delta k_{t-i}^{CAN} \end{pmatrix} + \begin{pmatrix} \varepsilon_t^{EW} \\ \varepsilon_t^{CAN} \end{pmatrix} \tag{A.4}$$

Bibliography

D. W. Andrews, "Tests for parameter instability and structural change with unknown change point," *Econometrica*, vol. 61, pp. 821–856, 1993.

D. W. Andrews and W. Ploberger, "Optimal tests when a nuisance parameter is present only under the alternative," *Econometrica*, vol. 62, pp. 1383–1414, 1994.

N. S. Balke and T. B. Fomby, "Threshold cointegration," *International economic review*, vol. 38, pp. 627–645, 1997.

A. J. Cairns, D. Blake, K. Dowd, G. D. Coughlan, and M. Khalaf-Allah, "Bayesian stochastic mortality modelling for two populations," *Astin Bulletin*, vol. 41, pp. 29–59, 2011.

L. R. Carter and R. D. Lee, "Modeling and forecasting us sex differentials in mortality," *International Journal of Forecasting*, vol. 8, pp. 393–411, 1992.

H. Chen, R. D. MacMinn, and T. Sun, "Mortality dependence and longevity bond pricing: A dynamic factor copula mortality model with the gas structure," *Working paper*.

S. H. Cox and Y. Lin, "Natural hedging of life and annuity mortality risks," *North American Actuarial Journal*, vol. 11, pp. 1–15, 2007.

S. H. Cox, Y. Lin, and S. Wang, "Multivariate exponential tilting and pricing implications for mortality securitization," *Journal of Risk and Insurance*, vol. 73, pp. 719–736, 2006.

I. L. Danesi, S. Haberman, and P. Millossovich, "Forecasting mortality in subpopulations using lee–carter type models: a comparison," *Insurance: Mathematics and Economics*, vol. 62, pp. 151–161, 2015.

G. Darkiewicz and T. Hoedemakers, "How the co-integration analysis can help in mortality forecasting," *DTEW Research Report*, vol. 0406, 2004.

H. M. Database, "University of california, berkeley (usa), and max planck institute for demographic research (germany)," 2015.

K. Dowd, A. J. Cairns, D. Blake, G. D. Coughlan, and M. Khalaf-Allah, "A gravity model of mortality rates for two related populations," *North American Actuarial Journal*, vol. 15, pp. 334–356, 2011.

R. F. Engle and C. W. Granger, "Co-integration and error correction: representation, estimation, and testing," *Econometrica*, vol. 55, pp. 251–276, 1987.

S. Gaille and M. Sherris, "Improving longevity and mortality risk models using common stochastic long-run trends," *UNSW Australian School of Business Research Paper*, vol. 2010ACTL13, 2010.

S. M. Goldfeld and R. E. Quandt, "A markov model for switching regressions," *Journal of econometrics*, vol. 1, pp. 3–15, 1973.

B. Hansen, "Testing for linearity," *Journal of Economic Surveys*, vol. 13, pp. 551–576, 1999.

B. E. Hansen, "Inference in tar models," *Studies in nonlinear dynamics & econometrics*, vol. 2, 1997.

B. E. Hansen and B. Seo, "Testing for two-regime threshold cointegration in vector error-correction models," *Journal of econometrics*, vol. 110, pp. 293–318, 2002.

P. R. Hansen, "Structural changes in the cointegrated vector autoregressive model," *Journal of Econometrics*, vol. 114, pp. 261–295, 2003.

L. Heligman and J. H. Pollard, "The age pattern of mortality," *Journal of the Institute of Actuaries*, vol. 107, pp. 49–80, 1980.

A. Hunt and D. Blake, "Modelling longevity bonds: Analysing the swiss re kortis bond," *Insurance: Mathematics and Economics*, vol. 63, pp. 12–29, 2015.

R. Ihle, S. von Cramon-Taubadel *et al.*, "A comparison of threshold cointegration and markov-switching vector error correction models in price transmission analysis," in *Paper presented on the NCCC-134 Conference on Applied Commodity Price Analysis, Forecasting and Market Risk Management, USA: St. Louis.* Citeseer, 2008.

S. F. Jarner and E. M. Kryger, "Modelling adult mortality in small populations: The saint model," *Astin Bulletin*, vol. 41, pp. 377–418, 2011.

S. Johansen, "Estimation and hypothesis testing of cointegration vectors in gaussian vector autoregressive models," *Econometrica*, vol. 59, pp. 1551–1580, 1991.

G. JONES, "Longevity risk and reinsurance," *Reinsurance News*, vol. 76, 2013.

M. Kijima, "A multivariate extension of equilibrium pricing transforms: The multivariate esscher and wang transforms for pricing financial and insurance risks," *Astin Bulletin*, vol. 36, pp. 269–283, 2006.

H.-M. Krolzig *et al.*, *Statistical analysis of cointegrated VAR processes with Markovian regime shifts.* Citeseer, 1996.

W. Kuo, C. Tsai, and W.-K. Chen, "An empirical study on the lapse rate: the cointegration approach," *Journal of Risk and Insurance*, vol. 70, pp. 489–508, 2003.

B. Larsen, "A threshold cointegration analysis of norwegian interest rates," *Thesis paper*, 2012.

D. Lazar, "On forecasting mortality using the lee-carter model," in *3rd Conference in Actuarial Science & Finance in Samos*, 2004.

R. D. Lee and L. R. Carter, "Modeling and forecasting us mortality," *Journal of the American statistical association*, vol. 87, pp. 659–671, 1992.

J. S.-H. Li and M. R. Hardy, "Measuring basis risk in longevity hedges," *North American Actuarial Journal*, vol. 15, pp. 177–200, 2011.

G. Listorti and R. Esposti, "Horizontal price transmission in agricultural markets: fundamental concepts and open empirical issues," *Bio-based and Applied Economics*, vol. 1, pp. 81–108, 2012.

D. Mitchell, P. Brockett, R. Mendoza-Arriaga, and K. Muthuraman, "Modeling and forecasting mortality rates," *Insurance: Mathematics and Economics*, vol. 52, pp. 275–285, 2013.

P. Newbold and C. W. Granger, "Experience with forecasting univariate time series and the combination of forecasts," *Journal of the Royal Statistical Society. Series A (General)*, vol. 137, pp. 131–165, 1974.

C. N. Njenga and M. Sherris, "Longevity risk and the econometric analysis of mortality trends and volatility," *Asia-Pacific Journal of Risk and Insurance*, vol. 5, 2011.

B. Seo, "Tests for structural change in cointegrated systems," *Econometric Theory*, vol. 14, pp. 222–259, 1998.

M. Stigler, "Threshold cointegration: overview and implementation in r," Working paper, Tech. Rep., 2010.

S. Wang, "Normalized exponential tilting: pricing and measuring multivariate risks," *North American Actuarial Journal*, vol. 11, pp. 89–99, 2007.

S. Wills and M. Sherris, "Securitization, structuring and pricing of longevity risk," *Insurance: Mathematics and Economics*, vol. 46, pp. 173–185, 2010.

J. R. Wilmoth, "Computational methods for fitting and extrapolating the lee-carter model of mortality change," Technical report, Department of Demography, University of California, Berkeley, Tech. Rep., 1993.

C. Wilson, "On the scale of global demographic convergence 1950–2000," *Population and Development Review*, vol. 27, pp. 155–171, 2001.

S. S. Yang and C.-W. Wang, "Pricing and securitization of multi-country longevity risk with mortality dependence," *Insurance: Mathematics and Economics*, vol. 52, pp. 157–169, 2013.

R. Zhou, J. S.-H. Li, and K. S. Tan, "Economic pricing of mortality-linked securities in the presence of population basis risk," *The Geneva Papers on Risk and Insurance-Issues and Practice*, vol. 36, pp. 544–566, 2011.